Optics Letters

Ultrafast-laser-ablation-assisted spatially selective attachment of fluorescent sensors onto optical fibers

Vikram Kamaljith,[1,*] Michael G. Tanner,[1,2] Harry A. C. Wood,[3] Kerrianne Harrington,[3] Debaditya Choudhury,[1] Mark Bradley,[4] and Robert R. Thomson[1,2]

[1]SUPA, Institute of Photonics and Quantum Sciences, Heriot-Watt University, Edinburgh EH14 4AS, UK
[2]Queen's Medical Research Centre, University of Edinburgh, Edinburgh EH16 4TJ, UK
[3]Centre for Photonics and Photonic Materials, Department of Physics, University of Bath, Bath, UK
[4]School of Chemistry, University of Edinburgh, Joseph Black Building, Edinburgh EH9 3FJ, UK
*Corresponding author: vk1@hw.ac.uk

Received 22 October 2019; accepted 8 December 2019; posted 14 February 2020 (Doc. ID 381018); published 6 May 2020

A robust method to selectively attach specific fluorophores onto the individual cores of a multicore fiber is reported in this Letter. The method is based on the use of ultrafast laser pulses to nanostructure the facet of the fiber core, followed by amine functionalization and sensor conjugation. This surface-machining protocol not only enables precise spatial selectivity, but it also facilitates high deposition densities of the sensor moieties. As a proof of concept, the successful deposition of three different fluorophores onto selected cores of a multicore fiber is demonstrated. The protocol was developed to include attachment of a fluorescence-based pH sensor using the ratiometric carboxynapthofluorescein.

https://doi.org/10.1364/OL.381018

Optical fibers provide a powerful way to transport light into and out of the body in a minimally invasive manner. In the case of endoscopy, this capability can be used for imaging, but optical fibers can also be employed for sensing. In the latter case, light can be used to directly interrogate the local environment of sensors immobilized onto the distal end of the optical fiber, using modalities such as absorption [1,2], fluorescence [3,4], and Raman [5,6]. In addition, it can be used to read out the effect that the environment has on the sensor. These sensors can take many different forms, and they include functionalized gold-coated silica nano-spheres [5–7], fluorescent beads [7,8], and fluorescence polymer coatings [9–13].

Of all the sensor technologies available, fluorescence offers the widest variety of sensing modalities, and it can be used to interrogate physiological parameters including pH [3,4,12], and O_2 [10,14] and CO_2 concentrations [12]. With the aim of maximizing the information that can be provided to clinicians for biomedical applications, while minimizing the device size, an important goal is to load multiple sensors onto the distal end of the fiber in a manner that facilitates multiplexed sensing. One route to achieve this is to use a multicore fiber (MCF) and attach different sensors specifically to different cores [11]. A variety of approaches can enable this, including the immobilization of fluorescent beads into etched pits in the distal end of the fiber [8], but this approach does not allow controlled deposition of specific sensors onto specific cores. With this in mind, there is a strong pull to develop new sensor-loading protocols that are spatially selective, controllable, and repeatable.

In this Letter, a powerful new route to robustly deposit different sensor dyes onto different cores of an MCF is reported. Our protocol exploits the precision and flexibility of ultrafast laser surface ablation to fabricate micro and nano structures on the facet of the MCF [15,16], which in turn can accommodate robust sensor immobilization. We showcase the potential of the protocol by depositing multiple fluorophores onto preselected locations of an MCF and utilize these to develop an optical fiber pH sensor.

Three steps were required in our protocol to deposit a desired sensor onto a specific set of MCF cores: (i) surface machining, (ii) surface functionalization, and (iii) fluorophore attachment. This protocol was repeated each time a different sensor was to be deposited onto a different set of cores. The experimental methodology for each step in the protocol was as follows:

(i) Surface Machining: Surface ablation was performed using an ultrafast laser source (Menlo Bluecut) that generated ~360 fs pulses of plane-polarized 1030 nm light at a pulse repetition rate of 250 kHz. For all experiments, the pulse energy on the sample was set to 0.56 mJ, and a 0.4 numerical aperture (NA) lens was used to focus the ultrafast laser pulses onto the facet of the 19-core MCF (each core had a diameter of 19 mm and a numerical aperture of 0.3), which was mounted on computer-controlled x–y–z translation stages (Aerotech ABL). A ~20 mm × 20 mm square area

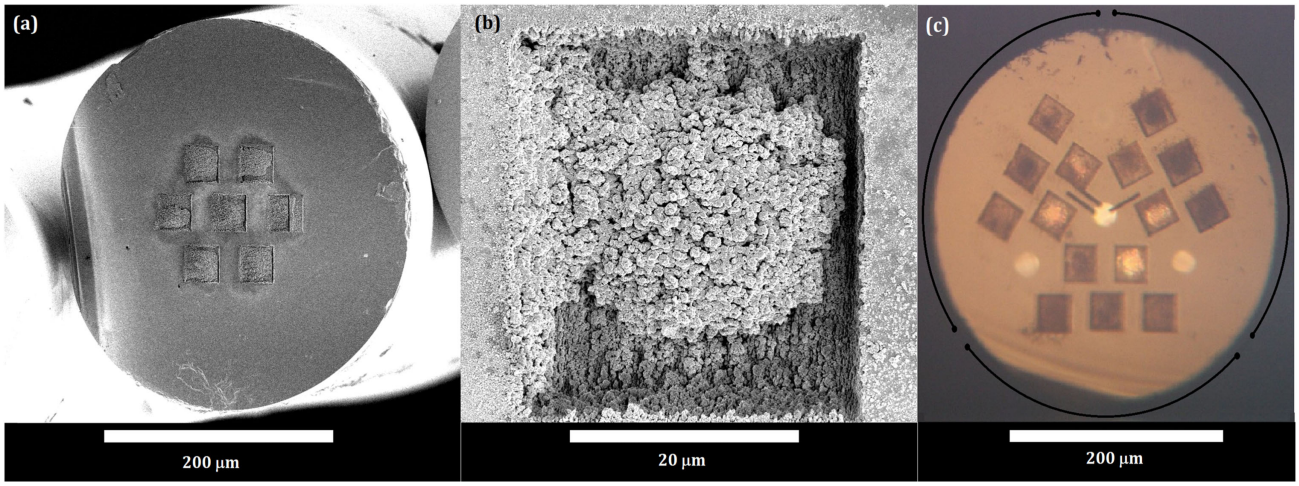

Fig. 1. Scanning electron microscope (SEM) images of the ultrafast laser-machined fiber end-facet: (a) the fiber facet and (b) magnification of one of the machined fiber cores. In (b), it can be seen that the round core and the surrounding cladding were ablated differently within the square-patterned region. Further cores were present in the fiber, but they were not ablated and are not visible in (a). (c) White light image of the facet of the machined MCF with multiple fluorophores deposited. Each 120° segment of the fiber facet (indicated in figure) had five processed cores with the same fluorophore deposited. The radial lines visible on the central core in (c) were machined to break the symmetry of the MCF to allow accurate multiple fluorophore deposition. The nonmachined cores are also visible.

on the facet of the specific core of interest was then ablated by translating the fiber past the laser focus in a raster pattern with a line separation of 1 μm and velocity of 20 $\mu m \cdot s^{-1}$. Scanning electron micrographs of the resulting features are shown in Figs. 1(a) and 1(b).

(ii) Surface Functionalization: Following ultrafast laser ablation, the fiber tips were submerged in a water sonicator for 10 min to remove any debris from the ablation sites, followed by rinsing with acetone. The cleaned fiber tips were then silanized in 20% of (3-aminopropyl)triethoxysilane in acetone. The silanization was performed for 4 h to ensure saturation of amine functionalization over the ablated silica surface. The fiber tips were then rinsed with acetone and air dried for 1 h.

(iii) Fluorophore Attachment: The amine functionalized fiber tips were treated with a solution of the active ester of the carboxyl derivative of the desired fluorophore. The fiber distal tip was placed in a 10 mM solution of the activated fluorophore in dimethylformamide (DMF) for 6 h to achieve saturation of the fluorophore attachment. Following fluorophore attachment, the tips of the fiber were placed into a sonicator bath in DMF for 3 min, and kept in DMF for 3 h to remove unattached fluorophore. This step became crucial when loading fluorescent molecules with significantly difference in quantum yields/extinction coefficients. Without this step, contamination from high-yield fluorophores was observed to flood the signal from lower-yielding counterparts.

These three steps were repeated each time a different fluorophore was attached to a different core(s). Apart from the minor reduction in fluorophore density, no notable changes in the fluorescence behavior of the dyes were observed after silanization and sonication.

Here we demonstrate the multiplexing potential of the protocol outlined above by depositing three different fluorescent molecules—5(6)-carboxyfluorescein (FAM) (Sigma-Aldrich), 5(6)-carboxynaphtho-fluorescein (CNF) (Sigma-Aldrich), and 5(6)-carboxytetramethyl-rhodamine (TAMRA) (ThermoFisher)—onto three separate sets of cores of a 19-core MCF. Out of the three fluorophores, both FAM and CNF had pH-dependent fluorescence spectral responses, whereas the pH-insensitive spectral response of TAMRA makes it an ideal candidate as a reference for ratiometric pH sensing. Figure 2 shows the proximal-end instrumentation used to interrogate the fluorescent sensors loaded onto the MCF at the distal end of the fiber. Lenses L1 and L2 were used to couple the 485 nm (Picoquant LDH-D-C-485) pump light into the MCF core of interest via a dichroic mirror (DM) (500 nm edge) and a band pass (BP) filter (460–490 nm) to pump the fluorescent dye at the distal end. The fiber transmitting the pump light from the laser (P1-405B-FC-1) exhibits a mode-field diameter of ∼3 μm at 480 nm. As such, when imaged onto the MCF (core diameter of 19 μm and core-to-core separation of 25 μm) with a magnification of 1, it enables precise coupling of pump light into individual cores of the MCF one at a time. The fluorescence from the loaded dye at the proximal end travels down the MCF core and is collected using lens L2, coupled through the long-pass DM and a long-pass (LP) (515 nm blocking edge) pump-blocking filter, and into a 50 μm-core multi-mode patch cable attached to a spectrometer (Ocean Optics, QE Pro). To minimize photo bleaching and ensure that the exposure conditions remain the same for each measurement, the laser diode and spectrometer were synchronized using a trigger signal generator, with which the pump exposure duration and time interval between measurements could be controlled.

To demonstrate the validity of our protocol, a 19-core MCF was loaded with 5(6)-carboxyfluorescein and 5(6)-carboxytetramethyl-rhodamine, as shown in Figs. 3(a) and 3(b). The fluorescence microscope images with the GFP filter clearly show the selective fluorophore deposition achieved using the laser ablation protocol. Using the proximal-end detection instrumentation, the spectral response of both the dyes to different pH buffers were measured before and after the fluorophore-loaded distal end of the MCF was treated with the

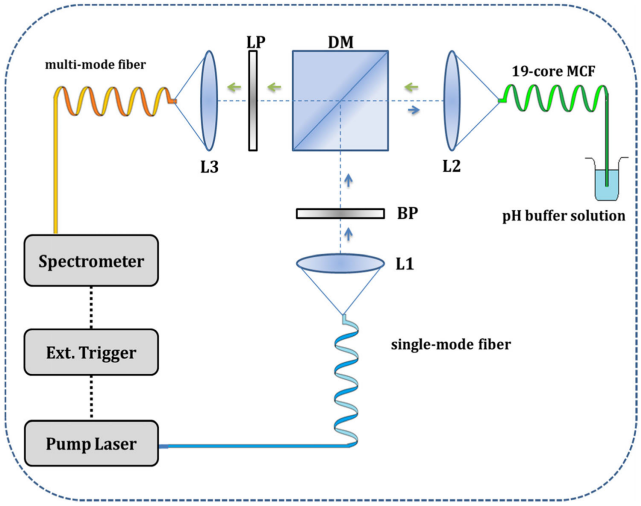

Fig. 2. Diagram of the proximal-end instrumentation for fluorescent signal acquisition.

silanization solution and sonicator bath in DMF. The spectral response, shown in Figs. 3(c) and 3(d), provides evidence that the silanization and the DMF sonicator bath have a minimal effect on the optical and chemical behavior of the deposited fluorophores.

Using our spatially selective dye immobilization protocol, multiple different dyes (FAM, TAMRA, and CNF, in that order) were deposited onto a 19-core silica MCF. The fluorescence emission was found to vary by approximately two orders of magnitude between FAM, TAMRA, and CNF, which here is primarily owing to the difference in quantum yield of these fluorophores. As shown in Fig. 1(c), each of the three fluorescent dyes were deposited onto a subset of five cores out of the 19. Owing to the otherwise symmetric core arrangement, surface machining was also performed around the central core to break the core symmetry during the fiber fabrication procedure, Fig. 1(c). Fluorescence spectra were obtained from one core of each functionalized set on the MCF, using the system shown in Fig. 2, at a pump power of 17 μWatt and an exposure time of 200 ms. To enhance the fluorescence yield and showcase the spectral difference between FAM and CNF, the distal end of the fiber was kept immersed in pH 9.0 buffer solution. The spectra obtained from the different cores normalized to the peak count are shown in Fig. 4(a). Importantly, the deposited fluorophores were subjected to substantial abrasion against the tissue and other soft surfaces to test the robustness of the deposition sites, with little to no adverse effect on their performance. These results confirm the ability of our protocol to attach different fluorophores to different cores in a highly selective manner.

Although there are other site-selective moiety attachment protocols [13,17], a key advantage of our protocol is also the significant increase in the area of the modified silica surface, and it is interesting to note that the laser-modified doped core material appears to be significantly rougher than the laser-modified cladding material [Fig. 1(b)]. This phenomenon enabled us to achieve a fluorophore loading density $\sim 6-7$ times greater than attachment without machining, a figure estimated by comparing fluorescence count from multiple fluorophore-loaded MCFs with and without surface machining, which in turn allowed accommodation of sensor molecules with lower fluorescence quantum yields that would otherwise be discarded owing to low-signal strength. CNF is a prime example, as it has a single excitation, yet it shows dual emission with an isobestic point (near 640 nm) in fluorescence emission with a pKa of 7.6, making it an ideal candidate for biological pH sensing [18].

To demonstrate the potential of our approach for developing fiber-optic pH sensors, 100 mM buffer solutions of varying pH values from 5.75 to 9.00 were prepared using appropriate sodium phosphates and measured using a commercial pH meter (Mettler Toledo, SevenGo Duo Pro). During initial fiber sensor development experiments, we noticed that the spectral response from the CNF exhibited dimer-like behavior owing to high fluorophore loading density. To rectify this, we used benzoic acid (BA) as a passive filler, by preparing the fluorophore solution with CNF:BA in a ratio of 1:5.

The distal end of an MCF, with only CNF attached, was immersed in the buffer solution for 30 s, to allow the solution to contact well with the fluorophores on the highly porous machined silica surface. Fluorescence spectra were then obtained by pumping one of the MCF cores with 12.5 mW of 485 nm light for 400 ms. The ratio of the fluorescence in two bands (570 nm to 630 nm and 630 nm to 730 nm) was calculated and plotted against the measured pH. During initial

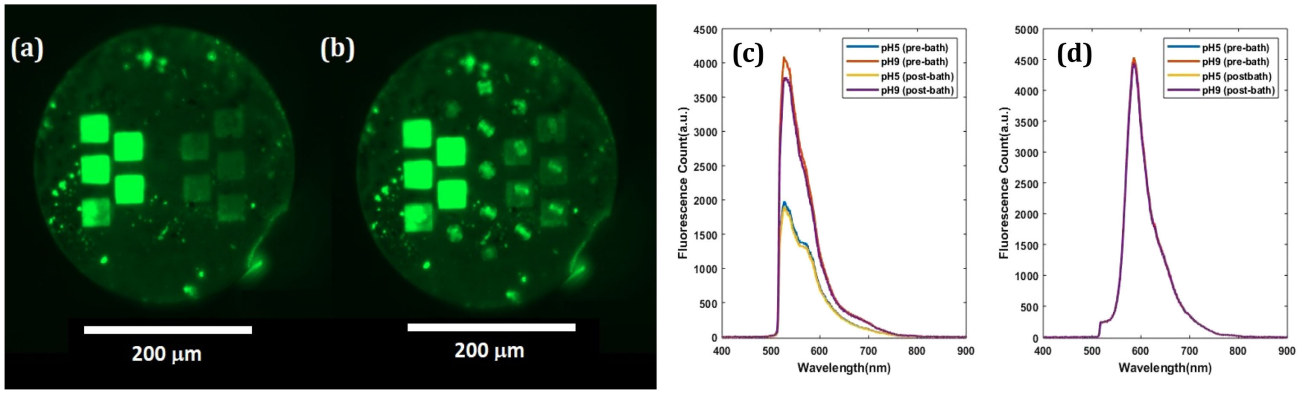

Fig. 3. Fluorescence microscope images of the 19-core MCF distal end, with targeted fluorophore loading of 5(6)-carboxyfluorescein on the right-hand side and 5(6)-carboxytetramethyl-rhodamine on left-hand side, under the GFP filter. To showcase the fiber core locations, images are captured (a) without and (b) with proximal-end illumination. The spectral response of (c) FAM and (d) TAMRA to pH5 and pH9 buffers before and after treatment with silanization solution and sonicator bath in DMF shows that these procedures have minimal impact on the deposited fluorophores.

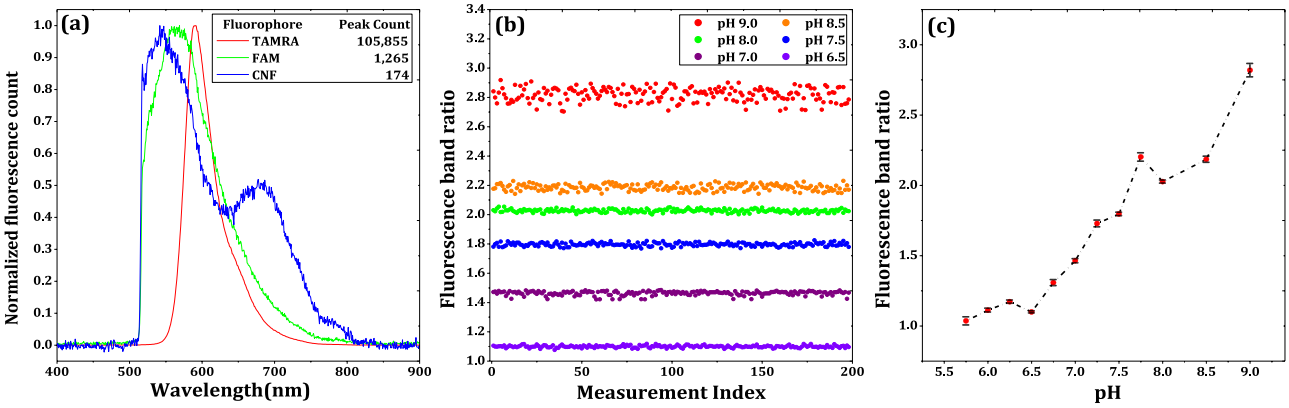

Fig. 4. (a) Fluorescence spectra measured from different cores of multiply loaded MCF, normalized to the peak count (shown in legend) of the respective spectra. (b) Fluorescence band ratio variation from fluorescence spectra obtained from the MCF loaded with CNF exposed to pH buffers ranging from 6.5 to 9.0, plotted against time over 190 consecutive measurements at a 20 s interval. (c) Variation of the fluorescence band ratio with respect to pH in the range of 6.0–9.0 for CNF on a single-fiber core.

experiments, we observed that the variability in the fluorescent band ratio was largely due to photo bleaching. To overcome this, we performed a preconditioning step that involved purposefully induced photo bleaching of readily attached fluorophores to reduce the fluorescence band ratio variability. Specifically, this preconditioning step involved illuminating the fiber core for 15 mins using 12.5 μWatts of pump power. To test and confirm the stability of the fluorescence band ratio, the preconditioned sensor was kept in one pH buffer, and measurements were taken for approximately 1 h at 20 s intervals. As shown in Fig. 4(b), no notable degradation of the sensor was observed during these measurements. The variation of the fluorescence band ratios with pH in the range of 5.75–9.00 is presented in Fig. 4(c). Data points represent an average of six measurements acquired at 5 s time intervals. This was repeated at different pH values (randomly ordered) for a total of five repetitions. In Fig. 4(c), data shown are the mean and standard deviation over the five randomized repeated measurements. Although we note that the fluorescence band ratio deviates from the overall trend at pH values 6.5 and 7.75, we also anticipate that the full spectral measurements will contains richer information about the fluorophore environment than is revealed by our ratiometric analysis and that this information can be used in the future to provide a more precise pH sensor.

In conclusion, we have demonstrated a new protocol based on ultrafast laser surface ablation that provides a versatile means to attach specific fluorophores to different cores of an MCF with high spatial selectivity. Furthermore, this protocol also results in a strong nano-structuring of the fiber surface, which increases the surface area and fluorophore loading density. This in turn provides a route to exploiting fluorophores that exhibit low fluorescence yields. In the future, this new protocol can enable miniaturized fiber-optic probes for multiplexed clinical sensing applications. Future work will pursue the implementation in biological sensing scenarios, as well as tailoring deposition protocols for the development of more complex detection schemes, such as multiplexed pH sensing and oximetry, and more advanced applications, such as enzyme activity detection.

Funding. Engineering and Physical Sciences Research Council (EP/K03197X/1).

Acknowledgment. The authors would like to thank Fuad Muhammad for useful discussions. Raw experimental data were made available through the Heriot–Watt University PURE research data management system [19].

Disclosures. The authors declare no conflicts of interest.

REFERENCES

1. L. W. Burgess, Sens. Actuators B **29**, 10 (1995).
2. R. Wolthuis, D. McCrae, E. Saaski, J. Hartl, and G. Mitchell, IEEE Trans. Biomed. Eng. **39**, 531 (1992).
3. M. Shortreed, R. Kopelman, M. Kuhn, and B. Hoyland, Anal. Chem. **68**, 1414 (1996).
4. D. M. Jordan and D. R. Walt, Anal. Chem. **59**, 437 (1987).
5. D. Choudhury, M. G. Tanner, S. McAughtrie, F. Yu, B. Mills, T. R. Choudhary, S. Seth, T. H. Craven, J. M. Stone, I. K. Mati, C. J. Campbell, M. Bradley, C. K. I. Williams, K. Dhaliwal, T. A. Birks, and R. R. Thomson, Biomed. Opt. Express **8**, 243 (2017).
6. C. Liu, S. Wang, G. Chen, S. Xu, Q. Jia, J. Zhou, and W. Xu, Sens. Biosensing Res. **1**, 8 (2014).
7. K. Wygladacz, A. Radu, C. Xu, Y. Qin, and E. Bakker, Anal. Chem. **77**, 4706 (2005).
8. K. L. Michael, L. C. Taylor, S. L. Schultz, and D. R. Walt, Anal. Chem. **70**, 1242 (1998).
9. M. J. Aernecke and D. R. Walt, Sens. Actuators B **142**, 464 (2009).
10. P. J. Rivero, J. Goicoechea, and F. J. Arregui, Polymers **10**, 280 (2018).
11. M. S. Purdey, J. G. Thompson, T. M. Monro, A. D. Abell, and E. P. Schartner, Sensors **15**, 31904 (2015).
12. J. A. Ferguson, B. G. Healey, K. S. Bronk, S. M. Barnard, and D. R. Walt, Anal. Chim. Acta **340**, 123 (1997).
13. F. Mohamad, M. G. Tanner, D. Choudhury, T. R. Choudhary, H. A. C. Wood, K. Harrington, and M. Bradley, Analyst **142**, 3569 (2017).
14. J. I. Peterson and R. V. Fitzgerald, Anal. Chem. **56**, 62 (1984).
15. T. Wei, Y. Han, H. Tsai, and H. Xiao, Opt. Express **33**, 536 (2008).
16. X. Lan, Y. Han, T. Wei, Y. Zhang, H. Tsai, and H. Xiao, Opt. Lett. **34**, 2285 (2009).
17. S. M. Barnard and D. R. Walt, Nature **353**, 338 (1991).
18. A. Song, S. Parus, and R. Kopelman, Anal. Chem. **69**, 863 (1997).
19. V. Kamaljith, M. G. Tanner, R. R. Thomson, and M. Bradley, Data supporting paper: Ultrafast laser ablation assisted spatially-selective attachment of fluorescent sensors onto optical fibres, doi: 10.17861/18427940-c9df-45d5-b90c-2eeac46f14ba (Heriot-Watt University, 2020).